Probing dark energy and inflation with 21cm line observations

Toyokazu Sekiguchi
(RESCEU, Univ of Tokyo)

JSPS-FAPESP workshop on dark energy, dark matter and galaxies
University of Sao Paulo, 19.02.2019

Plan of talk

- Introduction: 21cm line signals from IGM and minihalos
- Applications:
  - Primordial perturbations
  - Dark energy
- Summary

Refs:

- M. Kawasaki, TS, T. Takahashi [1104.5591]
- K. Kohri, Y. Oyama, T. Sekiguchi & T. Takahashi [arXiv:(1404.4847), (1303.1688), 1608.01601]
- (H. Tashiro, T. Sekiguchi & J. Silk, N. Sugiyama [arXiv:1311.3295])
- T. Sekiguchi, T. Takahashi, H. Tashiro & S. Yokoyama [arXiv:1705.00405,1807.02008]

Introduction

CMB last scattering $z \sim 10^3$

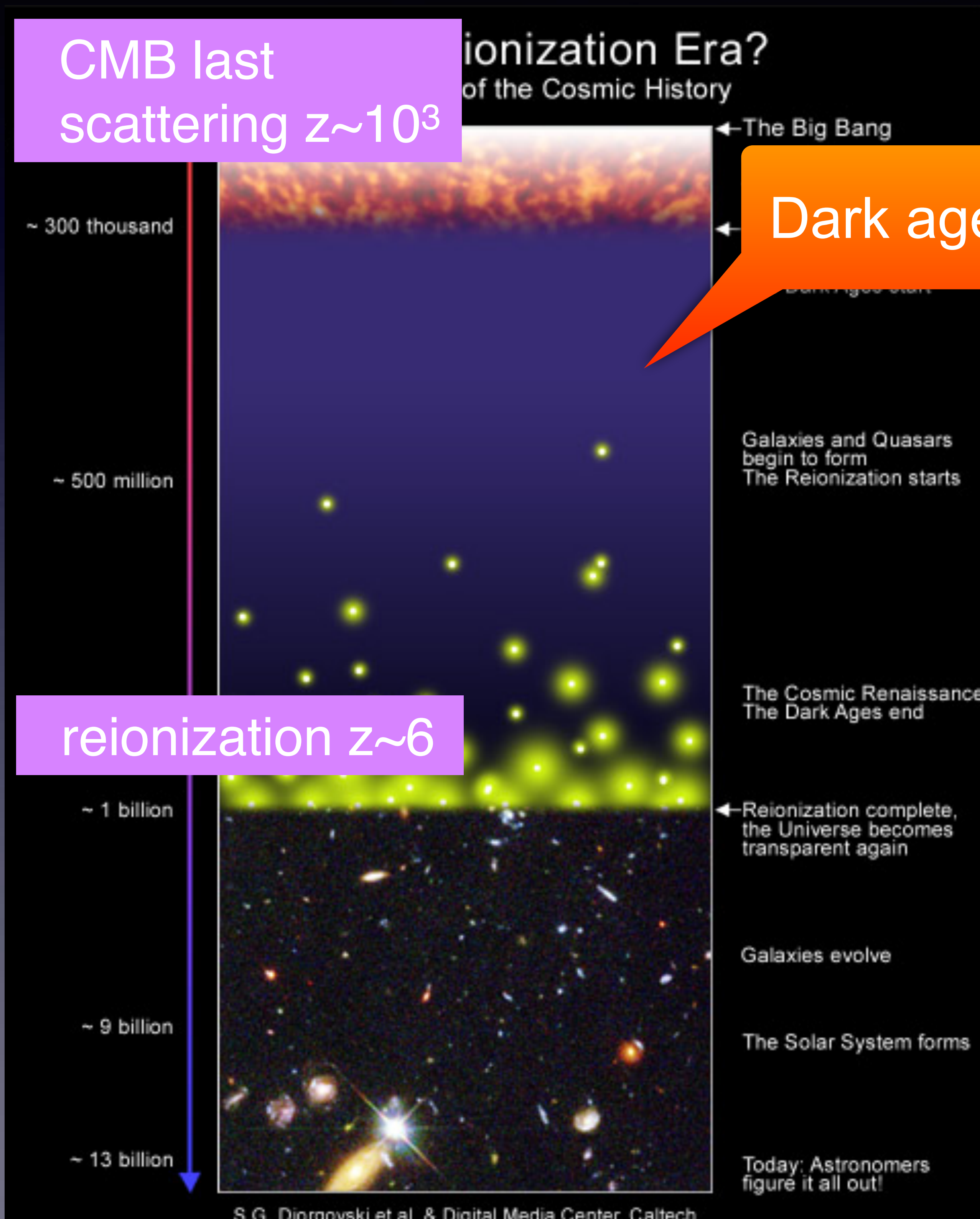

reionization $z \sim 6$

Dark ages (Epoch of reionization)

✓ neutral hydrogen

→ redshifted 21cm line

- tracer of matter fluctuations
- tomography → 3D mapping

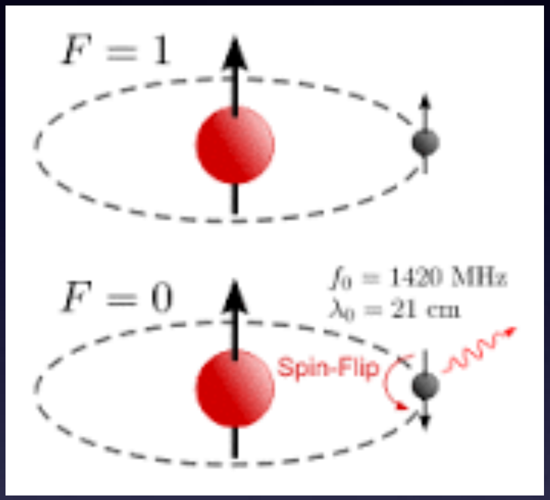

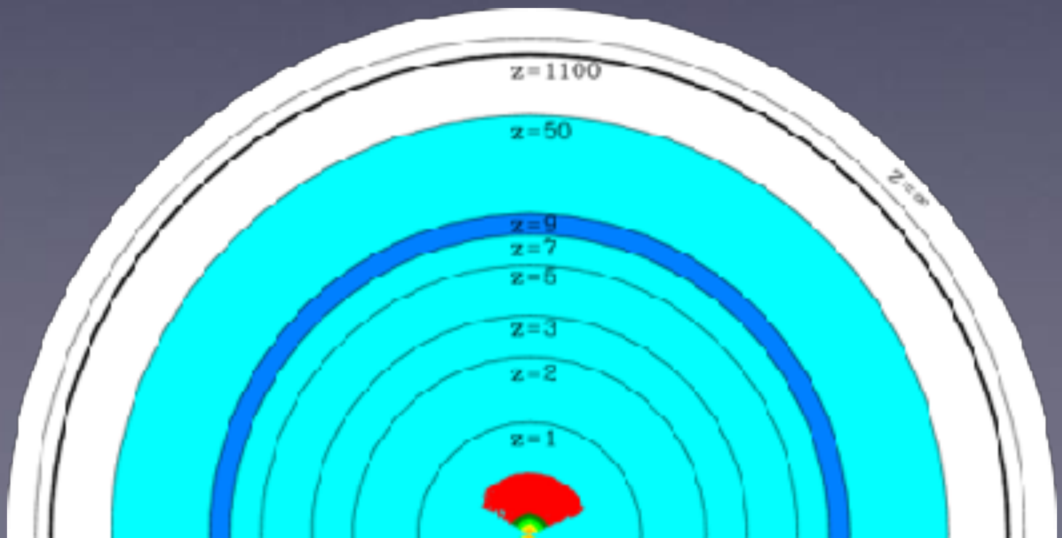

Mao+ '08

Redshifted 21cm line surveys

- Ongoing

  LOFAR, MWA, …

- Near future
  - ▸ Square Kilometer Array (SKA-low)
    - 21cm line from 3<z<27;
    - phase1 will start by 2023
  - ▸ Hydrogen Epoch Reionization Array (HERA)
    - main target: 21cm line from 7<z<12

- Far future

  FFTT, Omniscope, Lunar telescope?

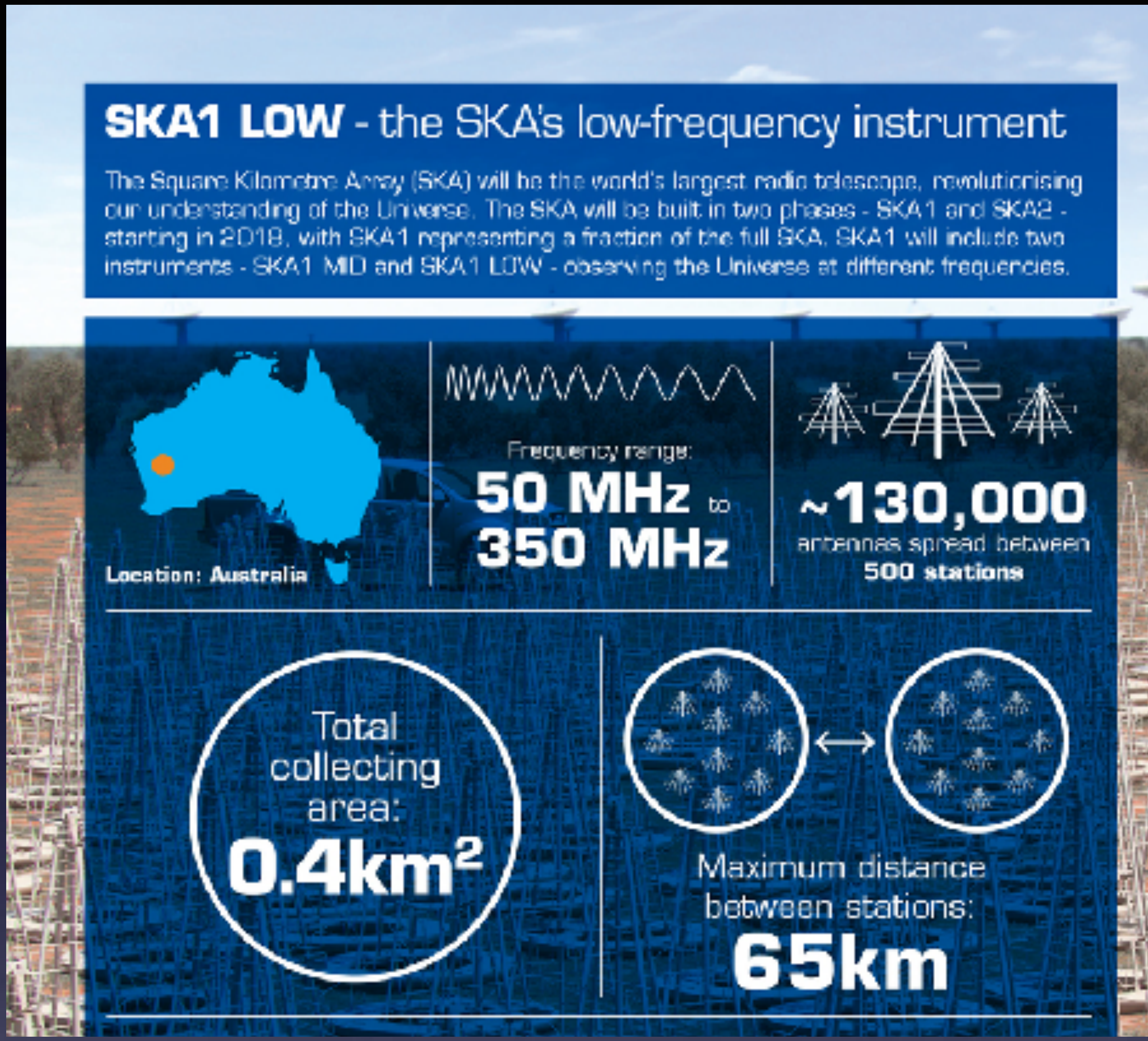

(c) www.skatelescope.org

What do 21cm surveys observe?

- Spin temperature
  - Ratio of triplets to singlet $n_{\rm triplet}/n_{\rm singlet} = 3\exp\left[-E_{\rm 21cm}/T_s\right]$

What do 21cm surveys observe?

- Spin temperature
  - Ratio of triplets to singlet $n_{\text{triplet}}/n_{\text{singlet}} = 3\exp\left[-E_{21\text{cm}}/T_s\right]$

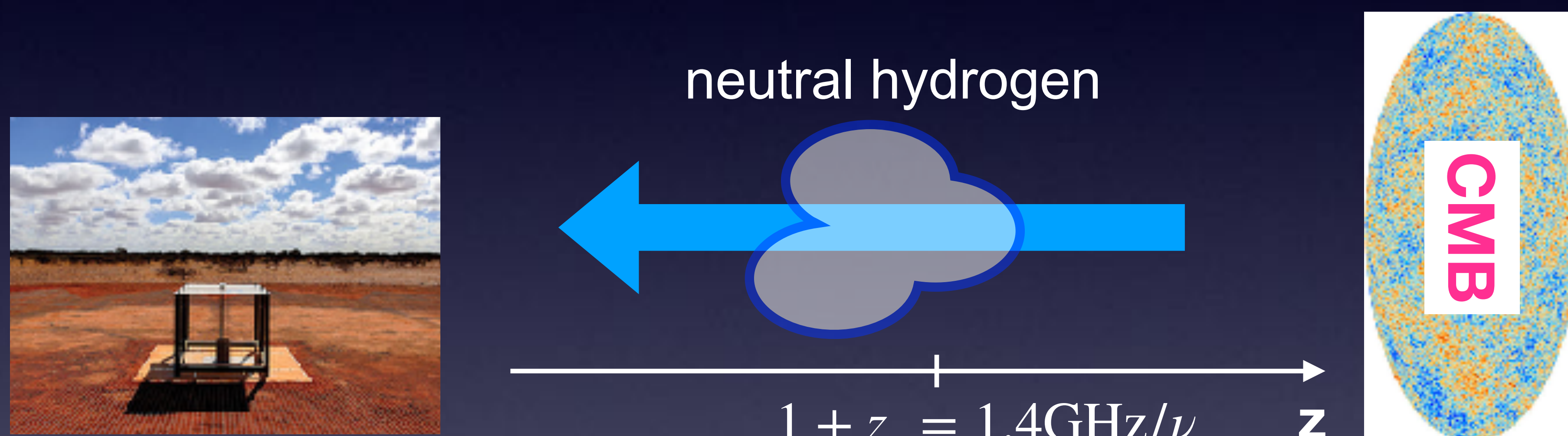

$$1 + z_\nu = 1.4\text{GHz}/\nu$$

- Brightness temperature
  - Radiative transfer

Emission if $T_s > T_{\text{CMB}}$

Absorption if $T_s < T_{\text{CMB}}$

$$T_{21\text{cm}}(\nu) = \frac{T_s(z_\nu) - T_{\text{CMB}}(z_\nu)}{1+z_\nu}\left(1 - e^{-\tau_{21\text{cm}}(\nu)}\right) \simeq (T_s - T_{\text{CMB}})\tau_{21\text{cm}}$$

  - 21cm optical depth $\tau_{21\text{cm}}(\nu) = \int dl \frac{3A_{10}\lambda_{21\text{cm}}^2}{32\pi}\frac{n_{\text{HI}}(z_\nu)}{T_s(z_\nu)}\phi(\nu)$

Sources of 21cm line

21cm fluctuation from IGM

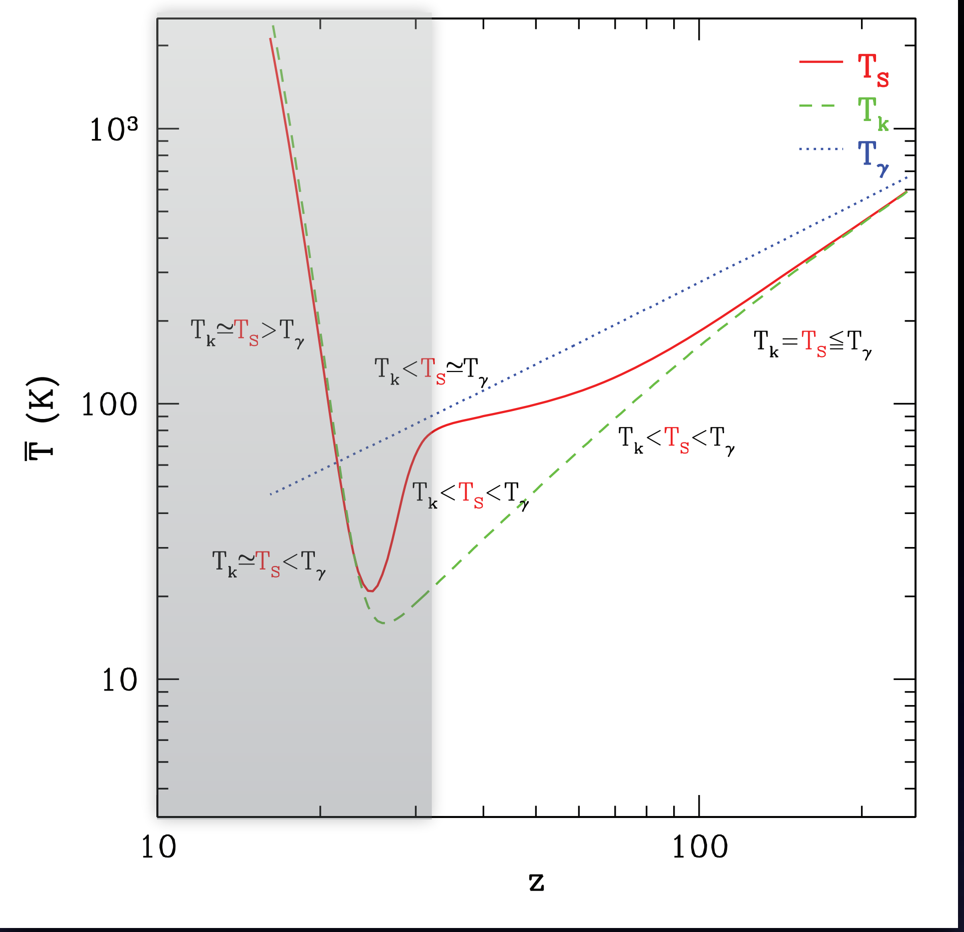

Messinger et al. 2011

- Differential brightness temperature

$$\Delta T_b = T_b - T_{\rm CMB} \simeq \frac{T_s - T_{\rm CMB}}{1+z}\tau_{21\rm cm}$$

At high redshifts z>20

(prior to formation of first objects), $T_s < T_{\rm CMB}$.

→ absorption

- Fluctuations in 21 cm brightness temperature

$$\delta_{21\rm cm} \approx \frac{\bar{T}_{\rm CMB}}{\bar{T}_s - \bar{T}_{\rm CMB}}(\delta_{T_s} - \delta_{T_{\rm CMB}}) + \delta_{n_{\rm HI}} - \frac{\hat{n}\cdot d\vec{v}_b/dr}{H}$$

$\mu = \hat{k}\cdot\hat{n}$

$\hat{n}$: line-of-sight direction

depends on δ_b

depends only on δ_m

isotropic

$\propto \mu^2$

21 cm can probe δ_b , separately from δ_m.

IGM 21cm power spectrum

- Tomographic power spectrum $\langle \delta T_b(\vec{k}) \delta T_b(\vec{k}') \rangle \equiv (2\pi)^3 \delta(\vec{k}_1 + \vec{k}_2) P(k_\parallel, k_\perp)$

$$\boxed{P(k_\parallel, k_\perp) = P_{\delta\delta}(k) + 2\mu^2 P_{\delta v}(k) + \mu^4 P_{vv}(k)} \quad k = \sqrt{k_\parallel^2 + k_\perp^2} \quad \mu = k_\parallel / k$$

- $P_{S_m}(k_0)/P_{\mathrm{AD}}(k_0) = 0.1$ at $k_0 = 0.0002\mathrm{Mpc}^{-1}$ $\quad z = 50,\ k_\parallel = 0.06\mathrm{Mpc}^{-1}$

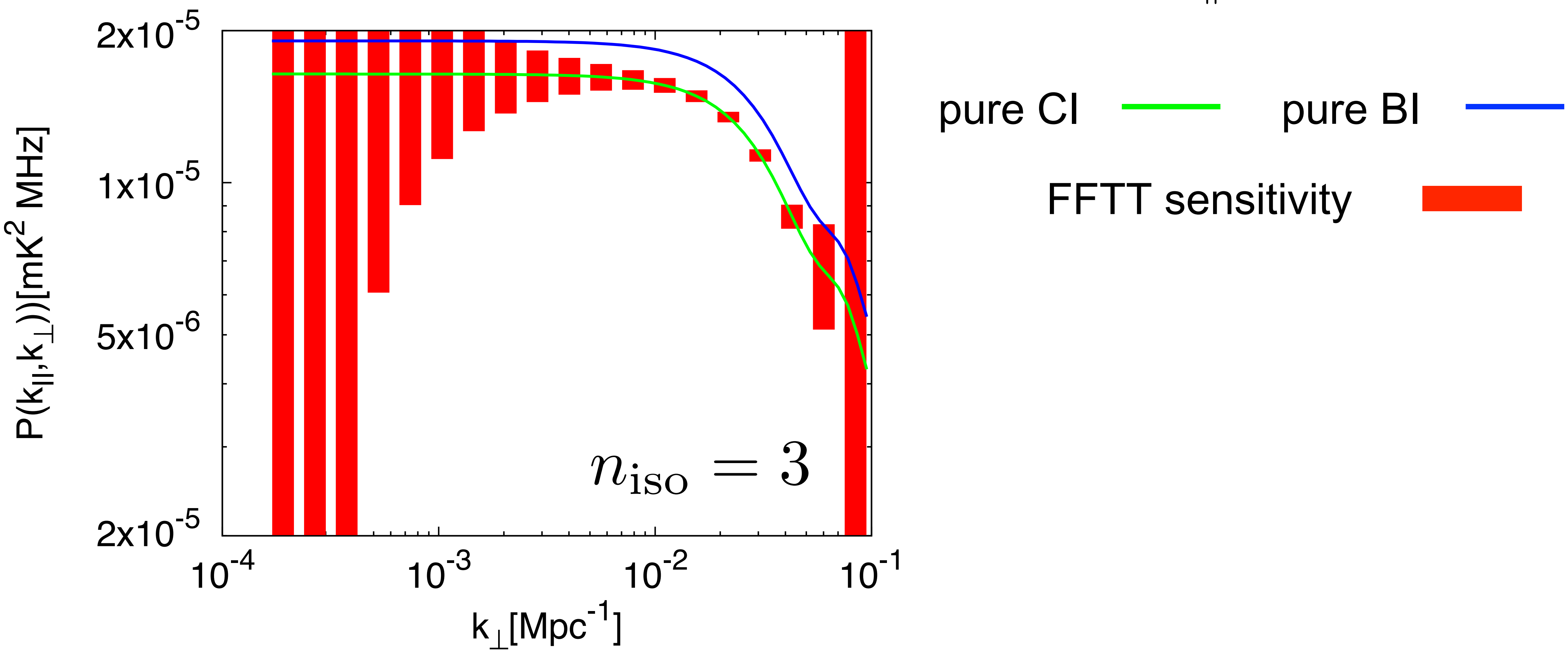

CDM/baryon isocurvature perturbation can be distinguished by 21cm.

Distinguishing CDM and baryon isocurvature

Kawasaki, TS, Takahashi 2011

- Fisher matrix analysis

$$r_{\rm CI} = P_{\rm CI}(k_0)/P_{\rm adi}(k_0),\ \ r_{\rm BI} = P_{\rm BI}(k_0)/P_{\rm adi}(k_0) \qquad k_0 = 0.002{\rm Mpc}^{-1}$$

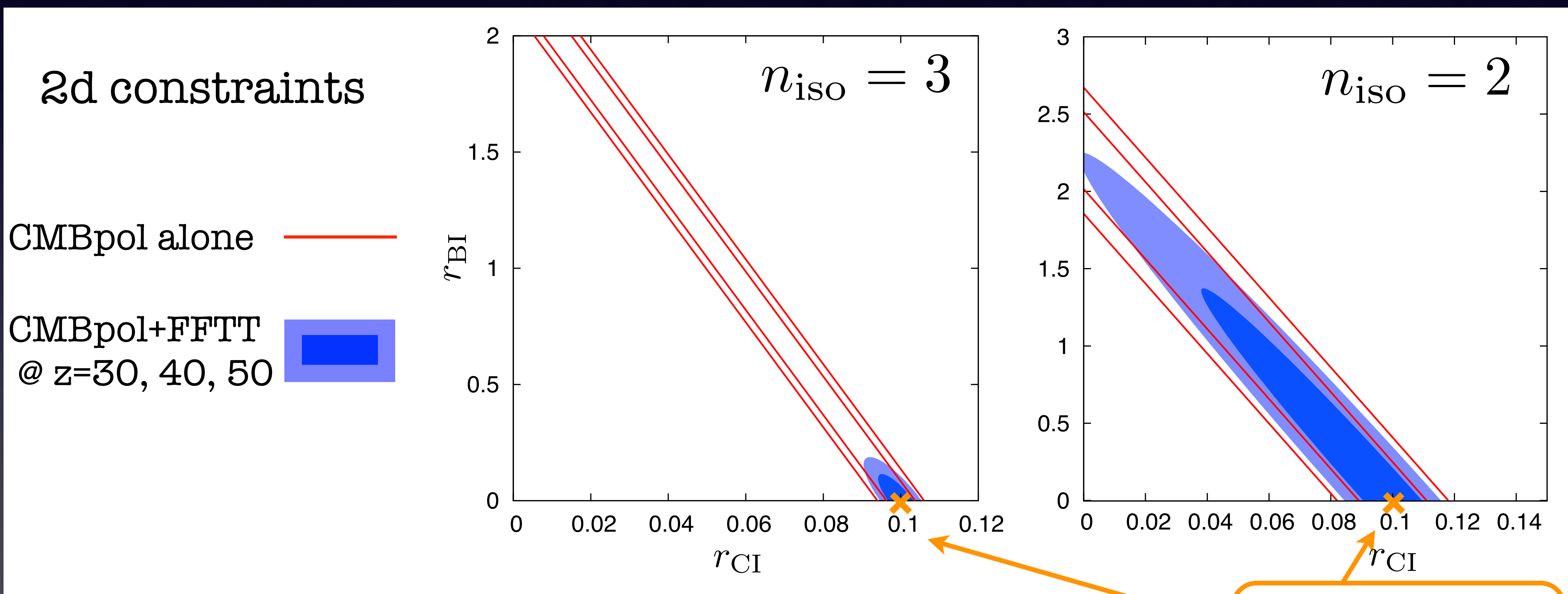

*fiducial model: pure CI

$(r_{\rm CI}, r_{\rm BI}) = (0.1, 0)$

Future 21 cm surveys can distinguish CI/BI if $n_{\rm iso} \gtrsim 2$.

Dark energy

Kohri, Oyama, TS, Takahashi 2017

Parameterized EoS

$$w(z) = w_0 w_1 \frac{a^p + a_s^p}{w_1 a^p + w_0 a_s^p} \approx \begin{cases} w_0 & (\text{for } a \gg a_s) \\ w_1 & (\text{for } a \ll a_s) \end{cases}$$

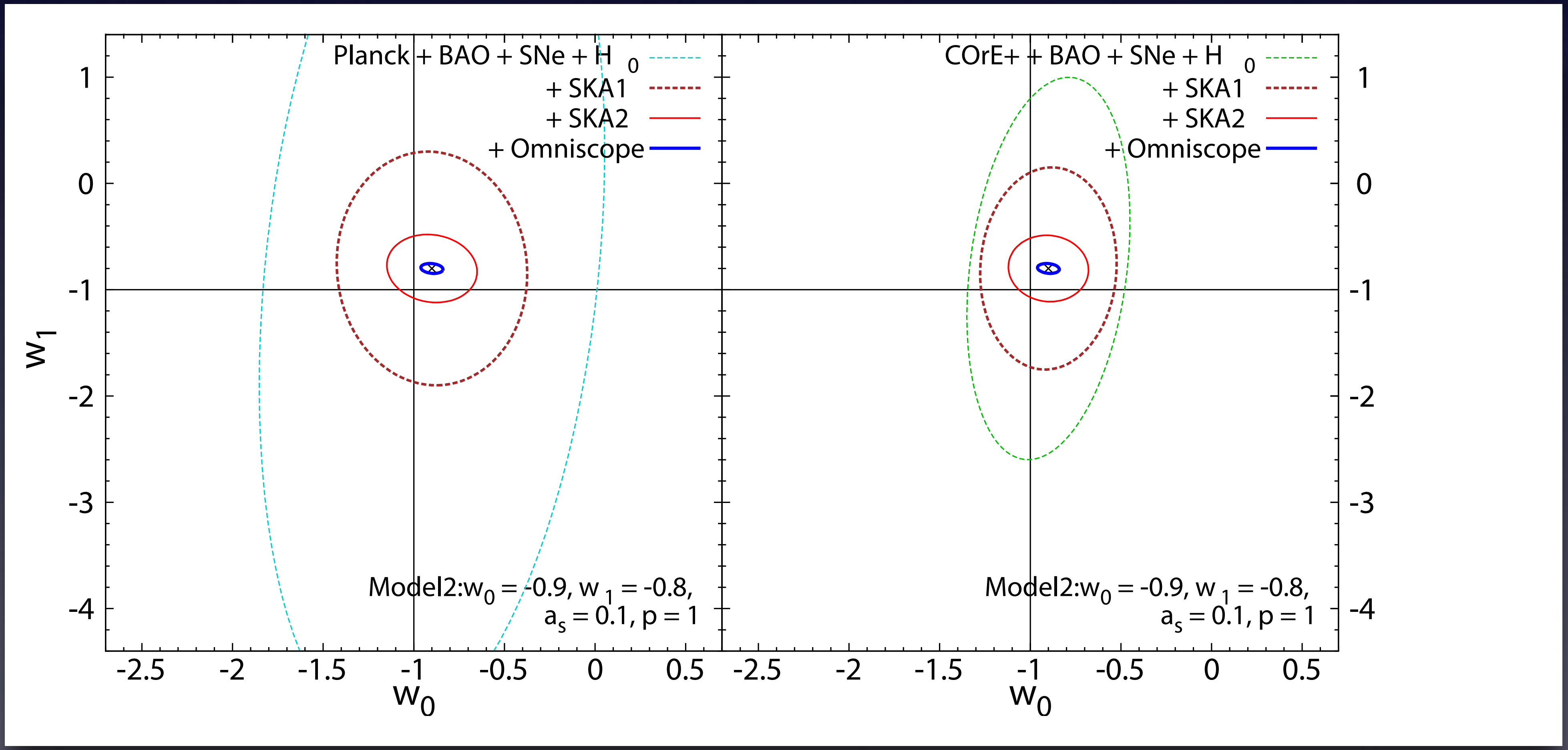

Redshifted 21cm line fluctuations can constrain early-type dark energy better than CMB.

Sources of 21cm line

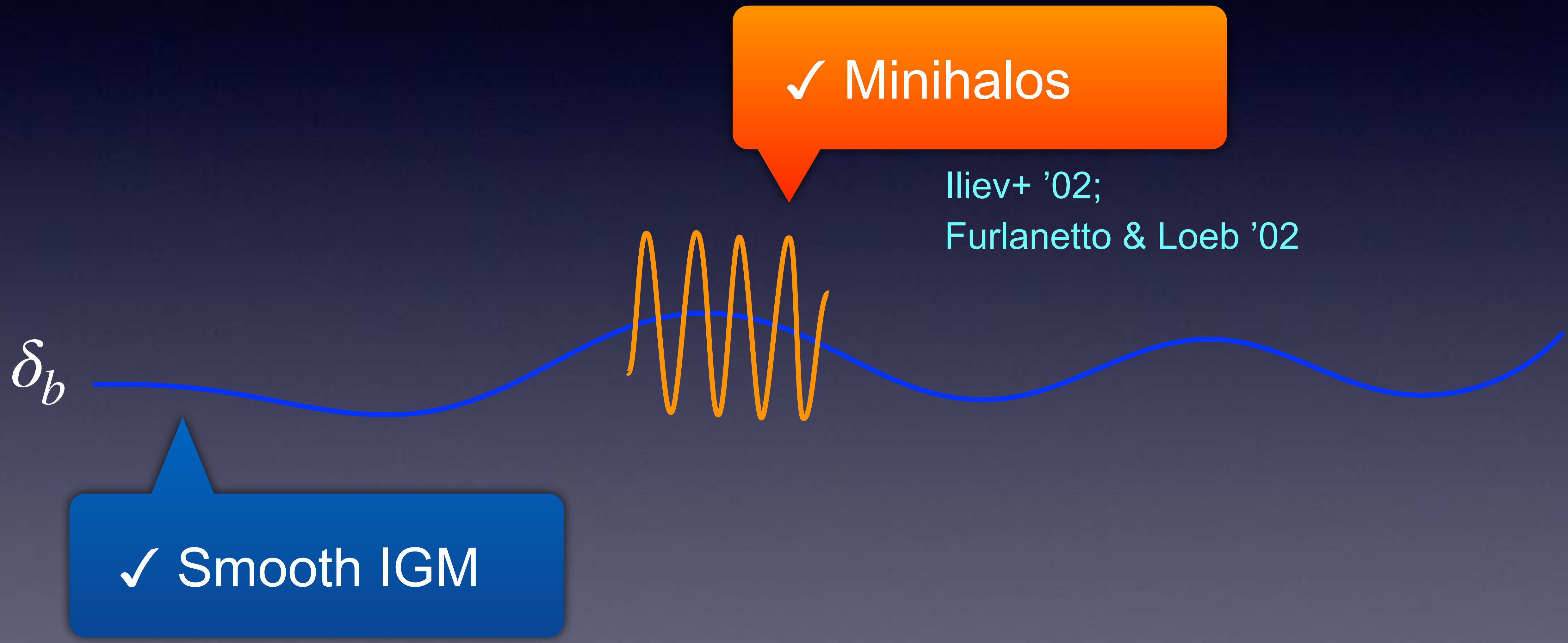

Minihalos

Halos too small to host galaxies

- No star formation: $T_{gas} < 10^4$K (inefficient radiative cooling)

  → dense neutral hydrogen inside; resistant to ionization

- Mass: $10^4 M_{sun} < M < 10^8 M_{sun}$

Sensitive to small-scale (<0.1Mpc) fluctuations

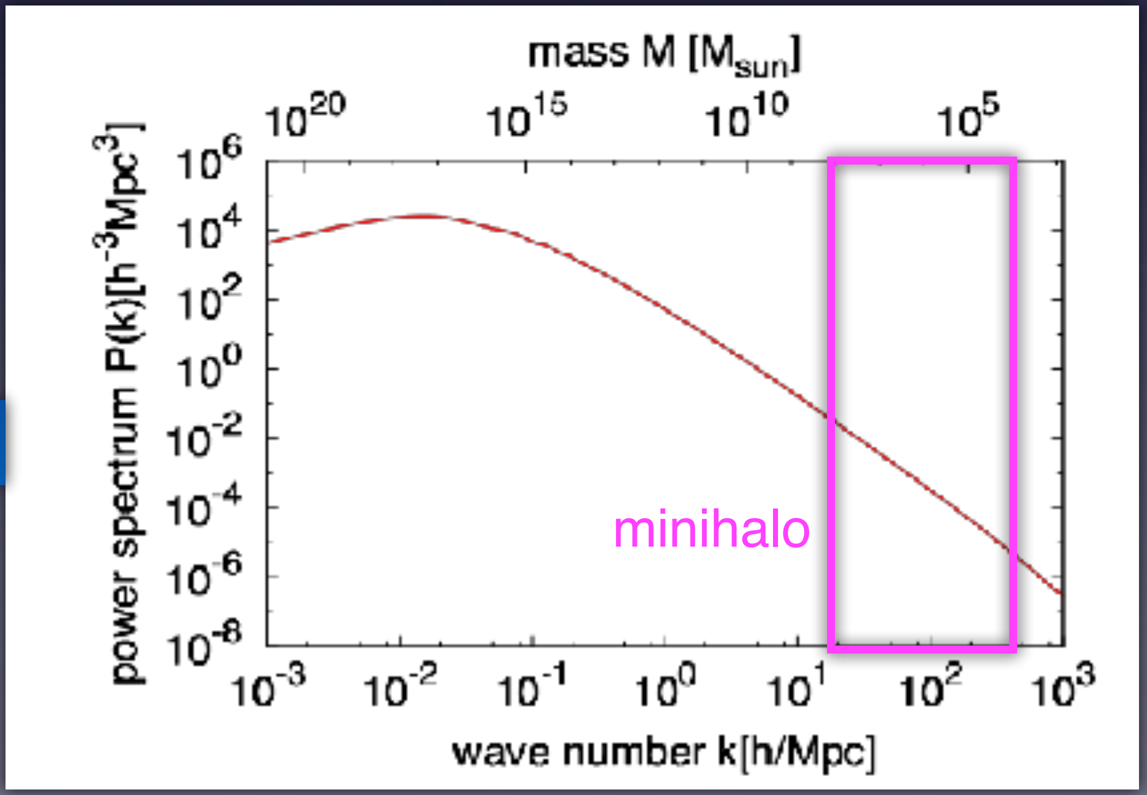

- Abundant, even at high-z

21cm line signal from minihalos

Iliev+ ’02;
Furlanetto & Loeb ’02

“21cm forest” in CMB

- Minihalos create emission/absorption features in CMB spectrum at radio frequency ν=1.4GHz/(1+z)

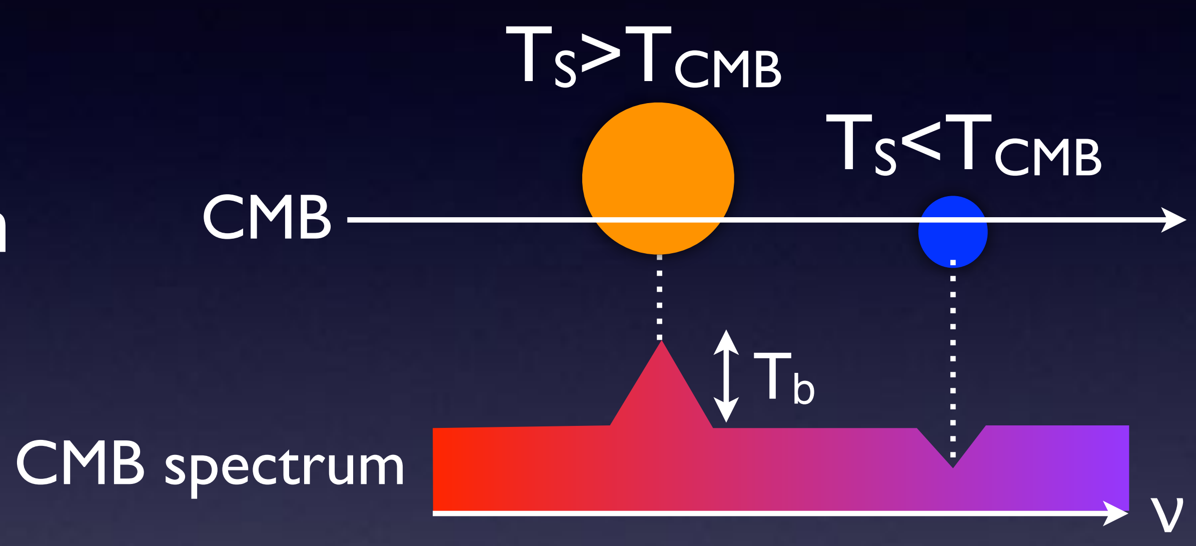

- Large (small) halos appear as emission (absorption)

- Individual halos are too small (size~kpc) to be resolved

  → intensity maps (like CMB)

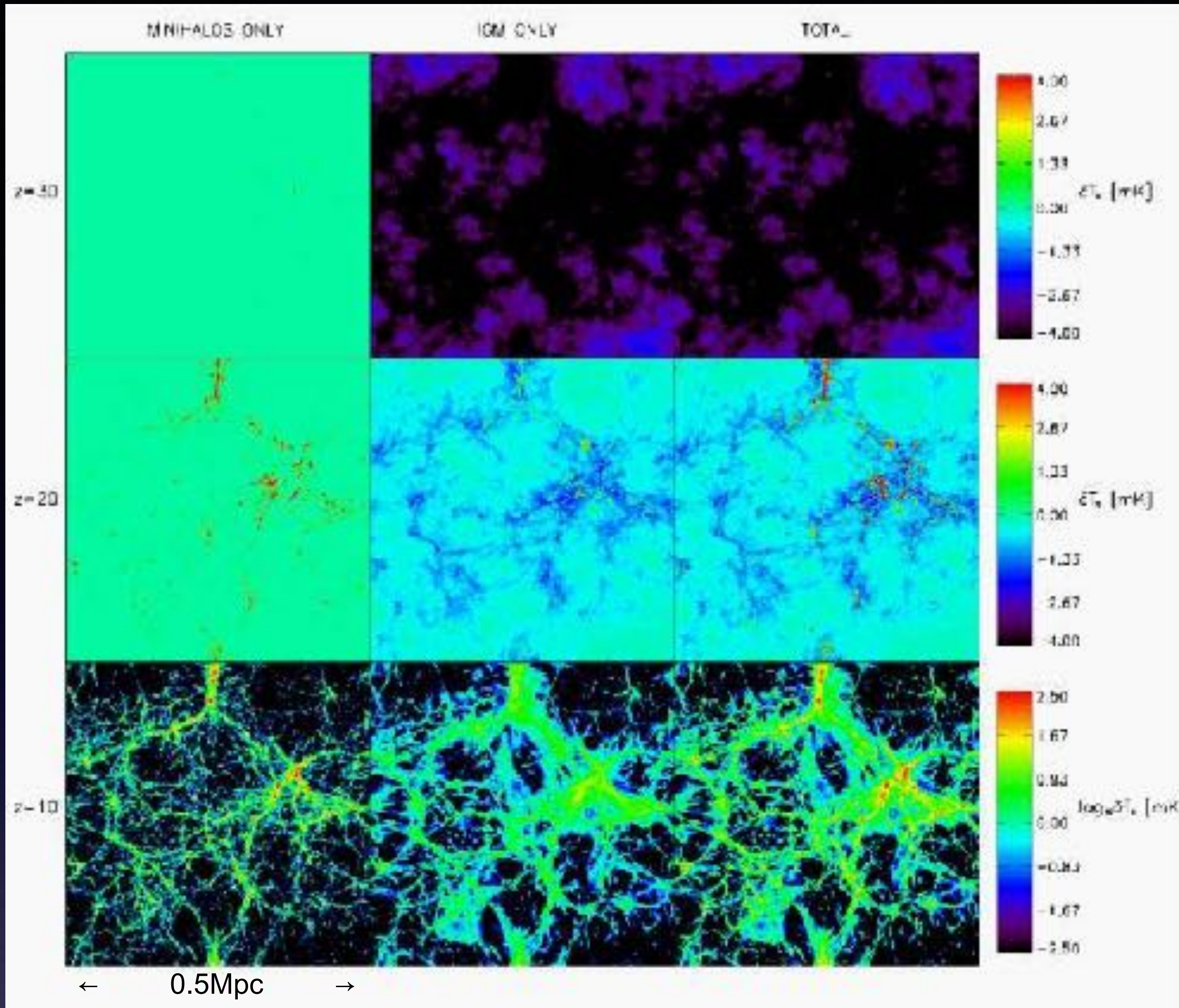

Simulations

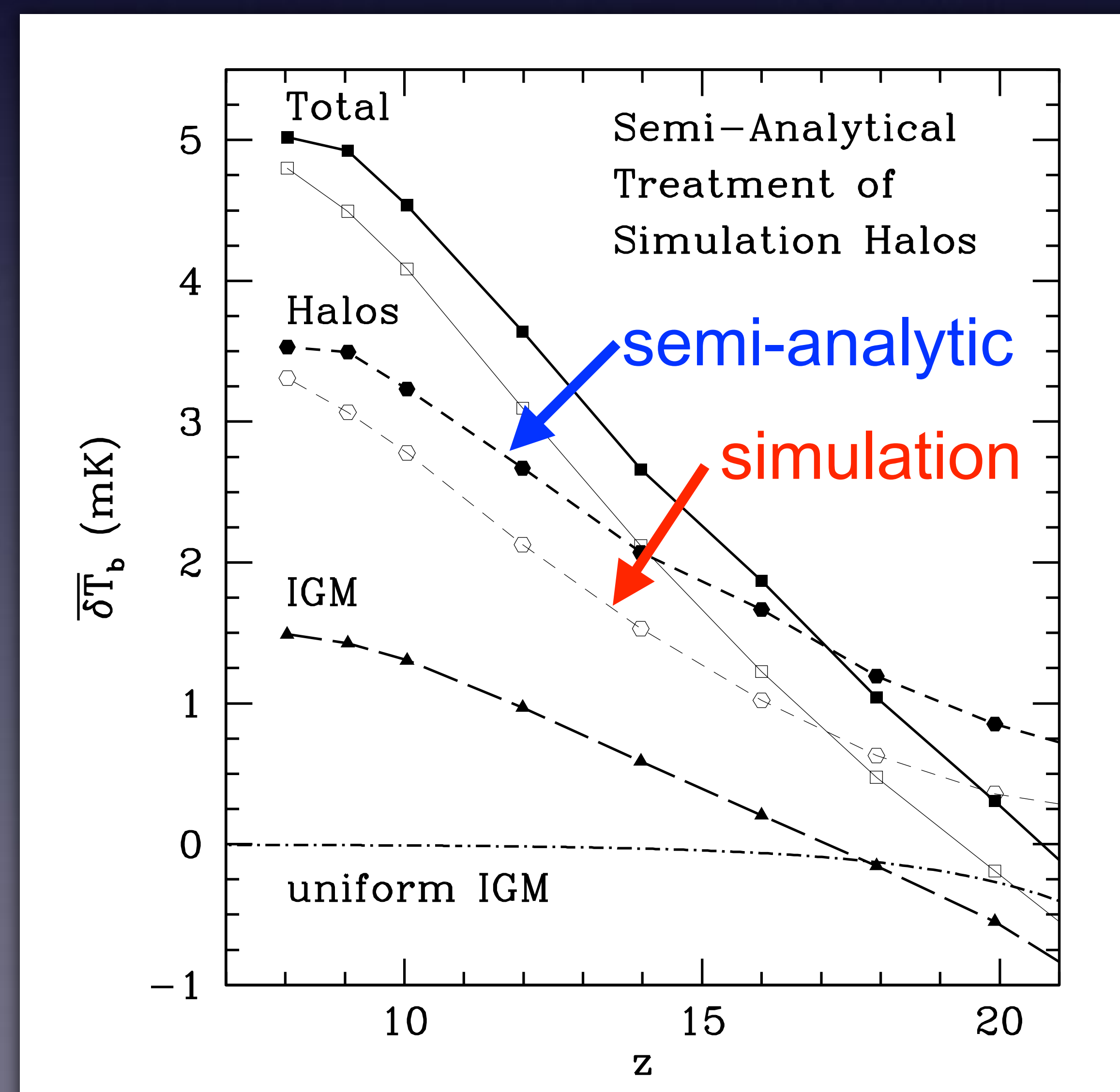

N-body+hydro simulations Shapiro+ '06

Minihalos can exceed the IGM around the epoch of reionization

Semi-analytical description agrees with simulations

21cm angular power spectrum from minihalos (1)

Iliev+ ’02; TS, Takahashi, Tashiro & Yokoyama ’17

Tomographic anisotropy (w/o redshift space distortion)

$$\delta T_b(\hat{n},\nu) = \left[\int_{M_{\rm min}}^{M_{\rm max}} dM \, \overbrace{T_b^{\rm (single)}(M,z_\nu) \frac{dN(M,z_\nu)}{dM}}^{\mathcal{F}_b(M,z)} b(M,z) \right] \delta(\vec{x}=r_\nu\hat{n},z_\nu)$$

- $T_b^{\rm (single)}(M,z_\nu)$: strength of 21cm line emission/absorption from single minihalo
- $\frac{dN(M,z_\nu)}{dM}$: mass function
- $b(M,z)$: halo bias
- mass function and halo bias: sensitive to small-scale (<Mpc) matter fluctuations
- $\delta(\vec{x}=r_\nu\hat{n},z_\nu)$: matter fluctuations at large scales (>Mpc)

21cm angular power spectrum from minihalos (2)

Iliev+ ’02; TS, Takahashi, Tashiro & Yokoyama ’17

Redshift-space distortion (Kaiser effect)

$$\delta T_b(\hat{n},\nu) = \overline{T}_b(z)\left[\beta(z) + f(z)\mu^2\right]\delta(\vec{x},z)$$

with $\mu = \hat{k}\cdot\hat{n}$

mean signal: $\overline{T}_b(z) = \int dM\, \mathcal{F}(M,z) = \int dM\, T_b^{(\mathrm{single})}(M,z)\frac{dN}{dM}(M,z)$

growth rate: $f(z) = d\ln D(z)/d\ln a$

flux-weighted effective bias: $\beta(z) = \frac{1}{\overline{T}_b(z)}\int dM\, \mathcal{F}(M,z) b(M,z)$

Tomographic angular power spectrum

$$C_l(z,z') = \frac{1}{2l+1}\sum_m a_{lm}(z) a^*_{lm}(z')$$

with $a_{lm}(z_\nu) = \int d\hat{n}\, \delta T_b(\hat{n},\nu) Y^*_{lm}(\hat{n})$

21cm angular power spectrum from minihalos (3)

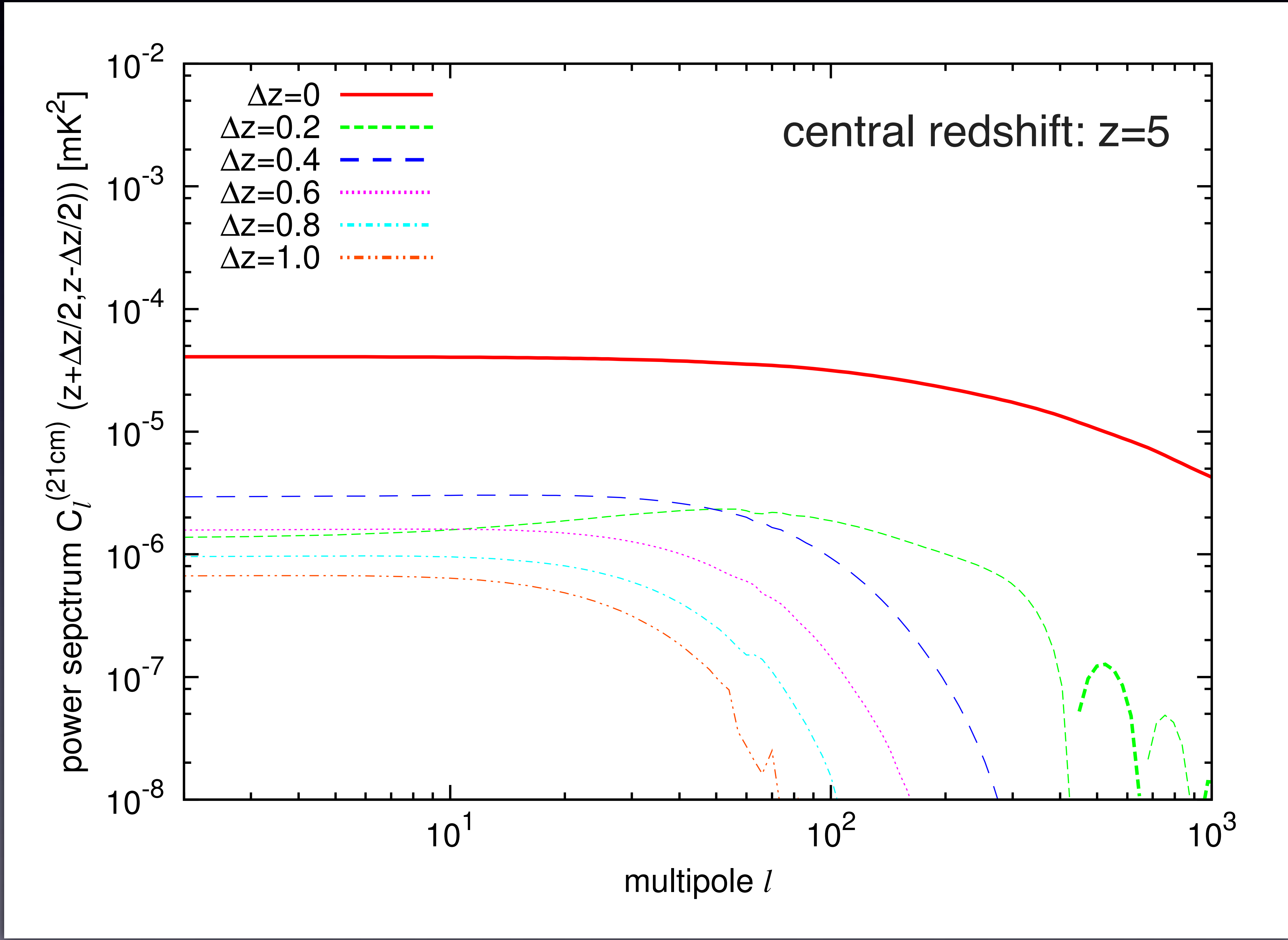

Application (1): Primordial spectral runnings

TS, Takahashi, Tashiro & Yokoyama [arXiv:1705.00405]

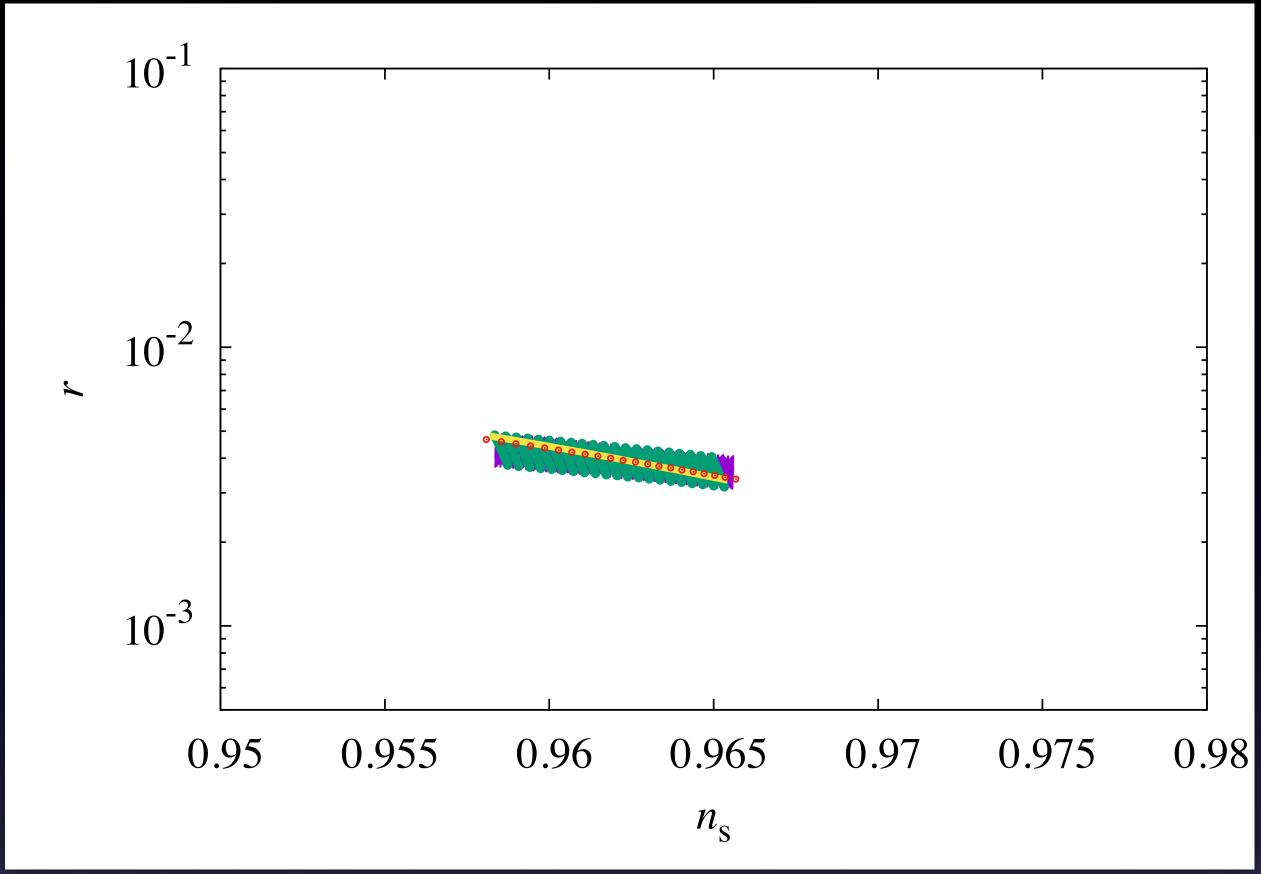

Spectrum of primordial fluctuations

$$\mathcal{P}(k) \propto k^{n_s - 1 + \frac{1}{2}\alpha_s \ln(k/k_*) + \frac{1}{6}\beta_s \ln^2(k/k_*) + \ldots}$$

- Many models degenerate in the n_s-r plane
- However, they can be distinguished from the scale dependence of n_s

Spectral runnings: a key observable for discriminating inflation models

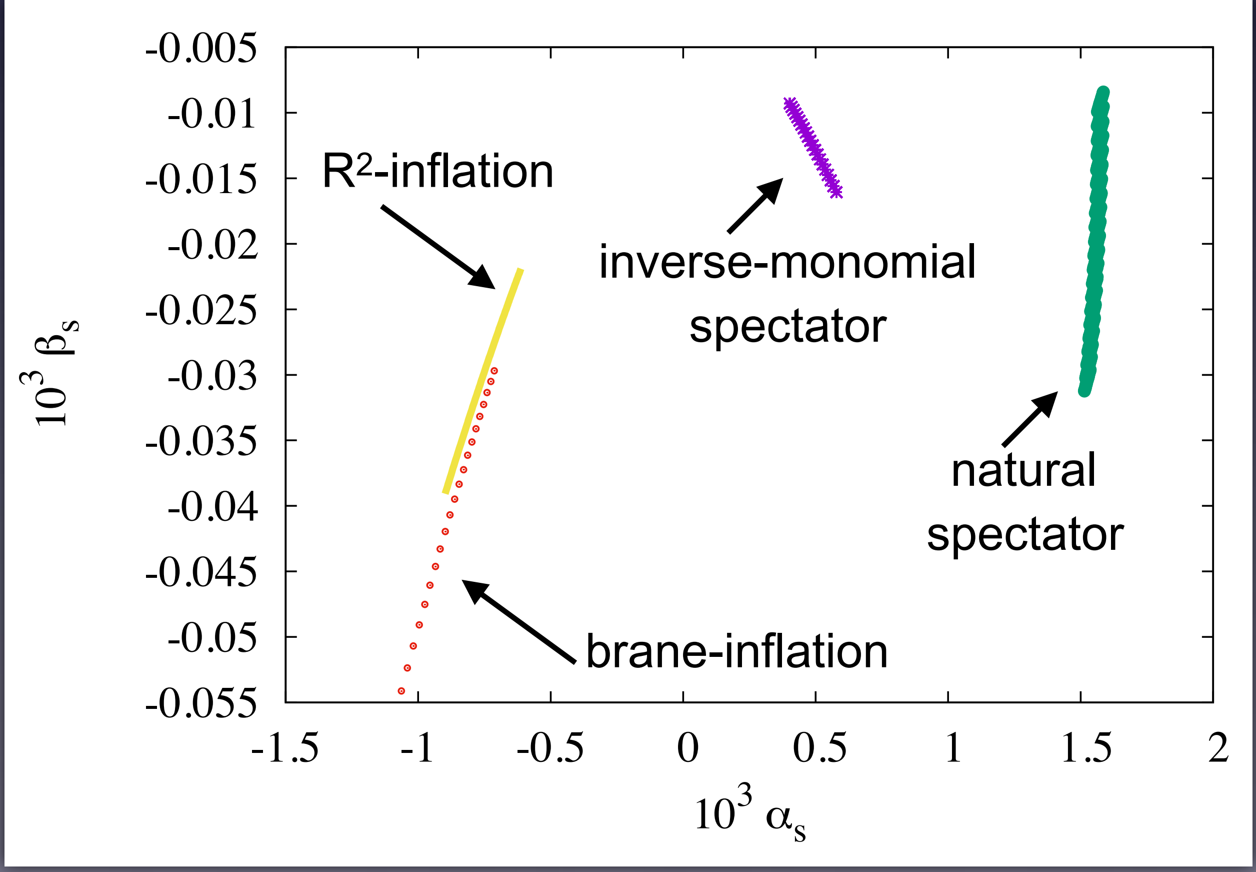

Application (1): Primordial spectral runnings (cont'd)

Parameter response

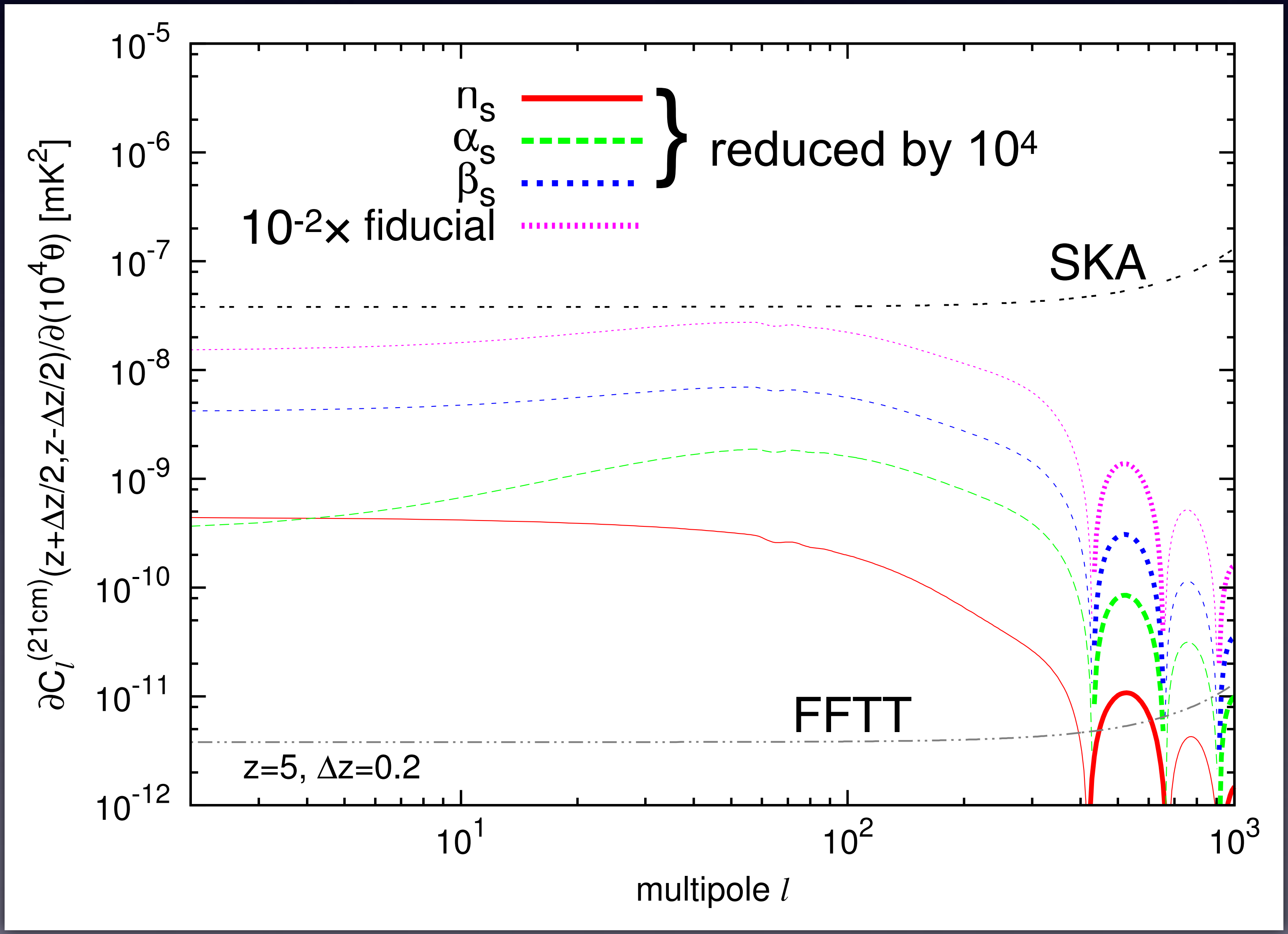

- Lower order spectral parameters (e.g. n_s or α_s) → spectral shapes
- Higher order parameters (e.g. β_s) → overall amplitudes

→ Solves parameter degeneracy

- Radial scale-dependence also enhances the discrimination

Application (1): Primordial spectral runnings (cont'd)

Forecasted constraints

Combination of CMB and 21cm is beneficial due to lever-arm effect.

$\Delta\alpha_s = 10^{-3}$, $\Delta\beta_s = 10^{-4}$

Constraints are dependent on z_{min} only mildly.

	$z_{\rm min}$	$10^{-3}\Delta n_s$	$10^{-3}\Delta\alpha_s$	$10^{-3}\Delta\beta_s$
Planck+SKA	4	1.4	1.4	0.40
	6	1.7	2.0	0.63
	8	2.3	3.0	0.85
	10	3.6	4.7	1.2
COrE+FFTT	4	0.85	0.96	0.24
	6	0.95	1.1	0.28
	8	1.0	1.2	0.31
	10	1.1	1.3	0.33

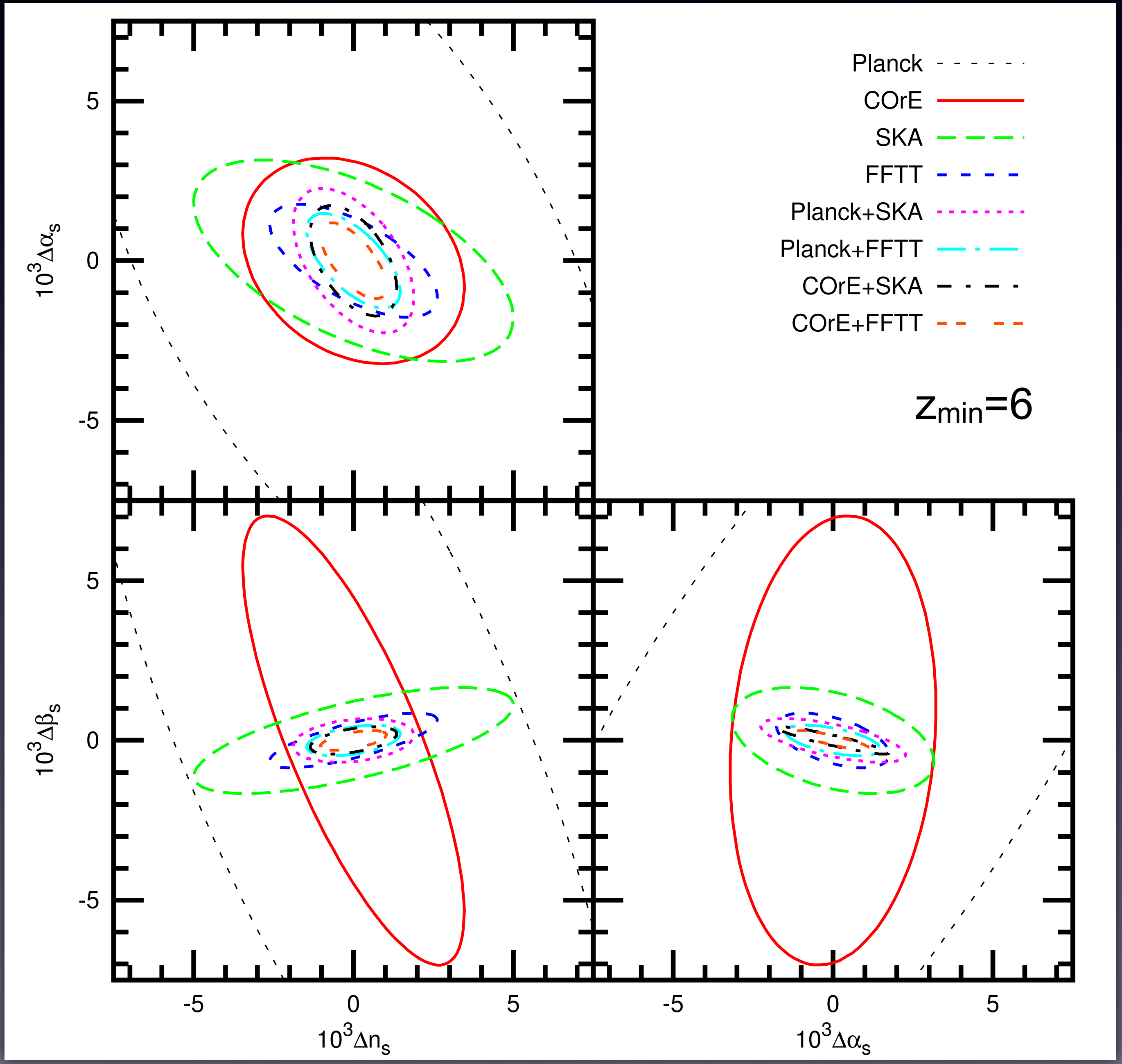

Application (2): Primordial non-Gaussianity

TS, Takahashi, Tashiro & Yokoyama, in prep.

Local type non-Gaussianity:

$$\Phi(\vec{x}) = \Phi_{\rm G}(\vec{x}) + f_{\rm NL}(\Phi_{\rm G}(\vec{x})^2 - \langle \Phi_{\rm G} \rangle^2) + g_{\rm NL}\Phi_{\rm G}(\vec{x})^3$$

- Small in single field inflation: f_{NL}~O(0.01), g_{NL}<O(10^{-3})
- Large in multi-field models (e.g. curvaton, modulated reheating, etc.)

Current tightest bound (Planck 2015)

$$f_{\rm NL} = 0.8 \pm 5.0, \quad g_{\rm NL} = (9.0 \pm 7.7) \times 10^4$$

cf. g_{NL}=(−3.3±2.2)×10^5 (WMAP 9yr)

TS & Sugiyama '13

Application (2):
Primordial non-Gaussianity (cont'd)

Effects of local-type non-Gaussianity on (mini)halos

- Correlation between large and small scale fluctuations
- relative halo # count $\frac{n_{\rm halo}}{\rho_m}(\vec{x})$ is modulated by large-scale fluctuations

→ scale-dependent halo bias Dalal+ '08; Slosar+ '08

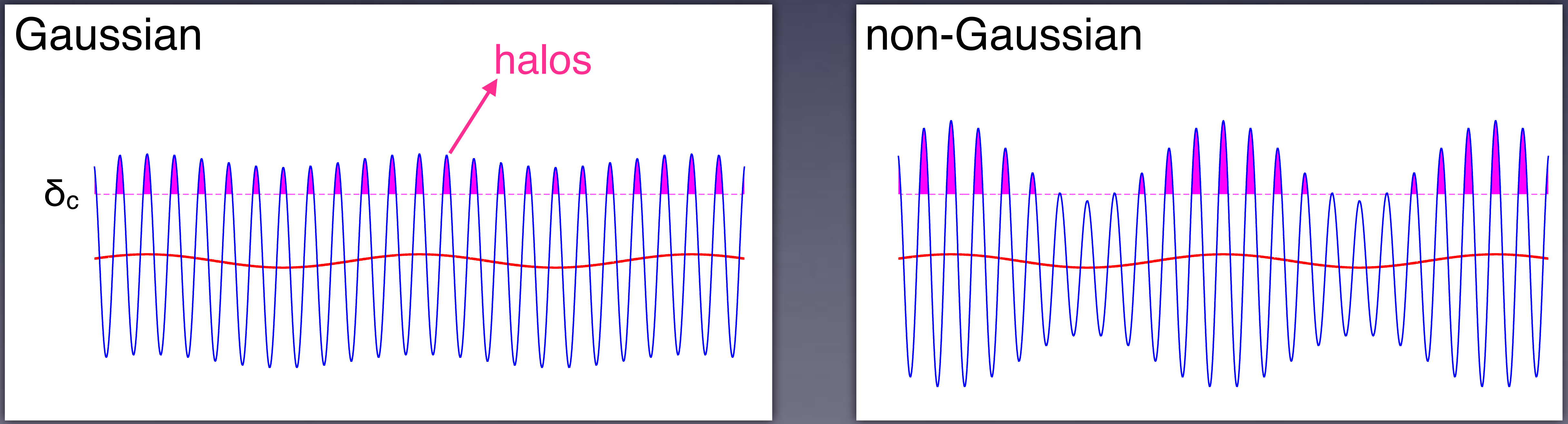

Application (2):
Primordial non-Gaussianity (cont'd)

Effects on minihalo power spectrum

Bias is more enhanced at larger scales

$$\Delta\beta(k,z) \approx \{\beta_f(z) f_{\rm NL} + \beta_g(z) g_{\rm NL}\} \frac{3\Omega_m H_0^2}{2k^2 T(k) D(z)}$$

→ 21cm line surveys are advantageous

✓ large transverse scale comparable to CMB

✓ cross-correlation of different redshifts

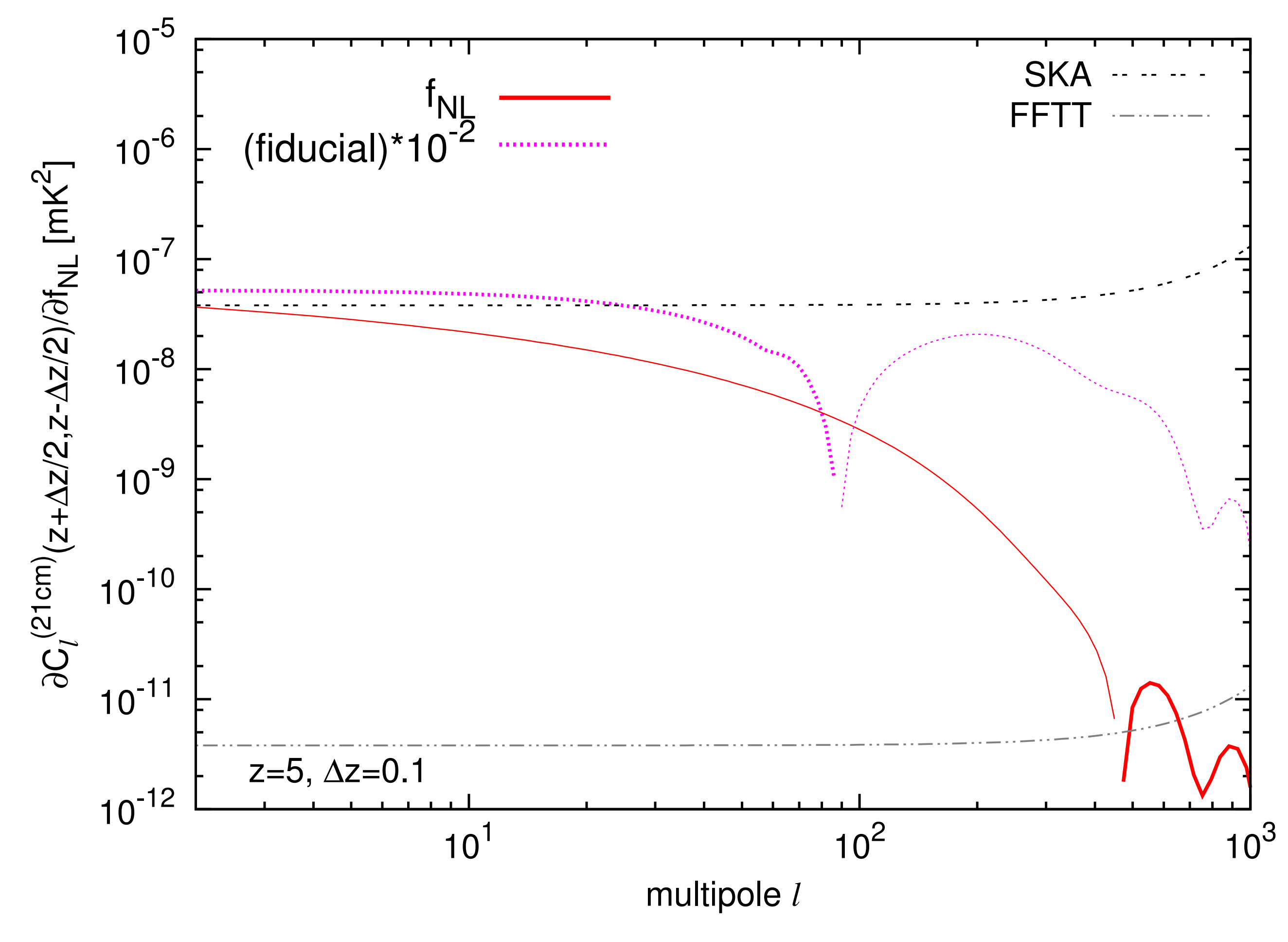

Application (2): Primordial non-Gaussianity (cont'd)

Forecasted constraints

Current CMB bound

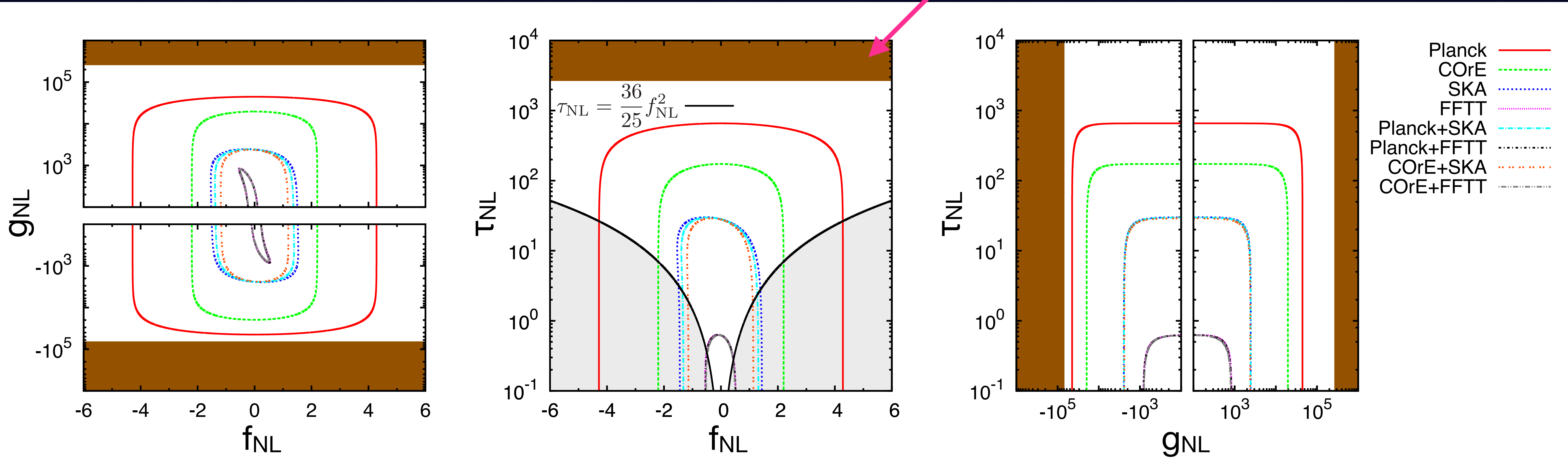

- Minihalos can improve the current (CMB) bound by orders of magnitude

$$\Delta g_{NL} \simeq O(10^3), \Delta \tau_{NL} \simeq O(10) \quad \text{(for SKA)}$$

- Suyama-Yamaguchi inequality can be tested

Application to dark energy

Constant EoS

- SKA: Δw ~ 0.05
- FFTT: Δw=0.02
- Cf. Planck: Δw=0.08

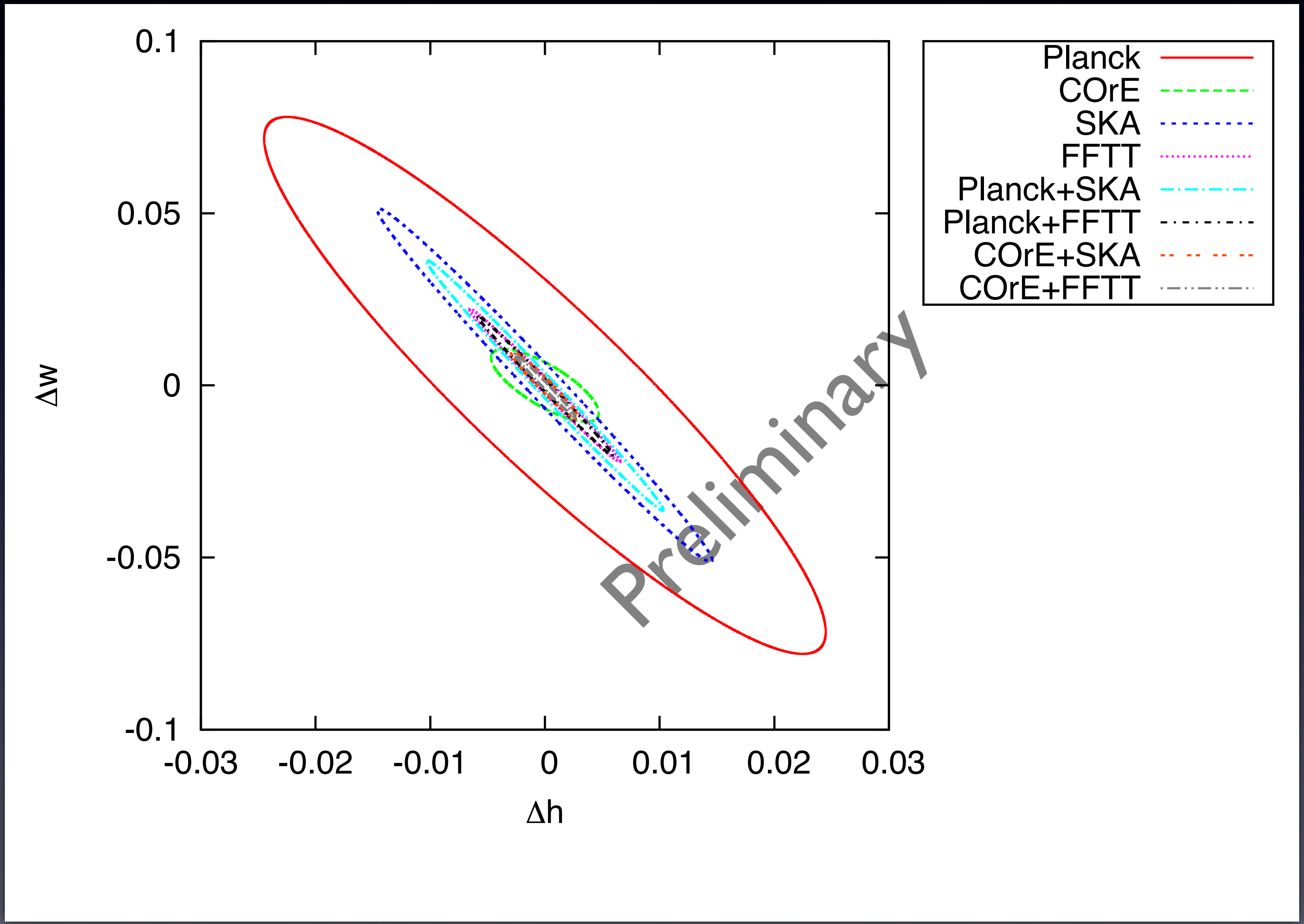

Both CMB and 21cm suffers from the degeneracy between w and the Hubble parameter.

Incorporation of direct Hubble measurements may be useful.

We will pursue our analysis with early-type DE in the future.

Summary

- High redshifted 21cm line fluctuations are a novel probe of the cosmological structure. There are largely two types of sources: smooth IGM and minihalos.
- Exploiting the tomographic nature of redshifted 21cm line fluctuations, we can constrain a variety of cosmological models.
    - Primordial fluctuations (spectral runnings, non-Gaussianity, etc.)
    - Dark energy
    - (DM, neutrinos, etc)